AC WAVEFORMS AND ELECTROMAGNETIC PROPERTIES

L. CAI
Solenoid Analyst, Formatter, Lab Technician

D. CHEN
Notebook Author, Editor, Lab Technician

R. LEW
Transformer Analyst, Lab Technician

J. LIN
RC/RLC Analyst, Editor, Lab Technician

V. WANG
RLC Analyst, Formatter, Programmer, Lab Technician

(Received 20 December 2017)

This experiment investigates the properties of alternating current in RC and RLC circuits, transformers, and solenoids. Phase shift in an RC circuit is found to be (77.263 ± .002)°, and an elliptical Lissajous figure is observed. Natural frequency in an RLC circuit is measured to a high degree of accuracy. Energy dissipation is observed in a transformer at high frequencies. Magnetic fields are measured and compared at various points near solenoids, and compared to a simulation written in MATLAB.

I INTRODUCTION

The dynamic nature of alternating current and its commonplace entices a curiosity into its structure which can be analyzed closely as internal compositions. Experiments which focus on the fundamental components such as RC and RLC circuits, and simple solenoid transformers build the foundation for understanding of the infrastructure. Furthermore, the inherent fields produced present an abstract and often unnoticed effect. The simulation of such phenomena present a better visualization for future studies.

II THEORY

AC circuits contain an alternating sinusoidal potential, which is a function of time.

$$V(t) = V_p \sin(\omega t - \phi) + k \qquad [1]$$

Where: *(HRW, 2010)*

V = Potential (V)
V_p = Potential amplitude (V)
ω = Angular frequency (rads^{-1})
t = Time (s)
ϕ = Horizontal shift (rad)
k = Vertical shift (V)

The theoretical potential current phase difference can be found by:

$$\phi = \tan^{-1} \frac{1}{2\pi f RC} \qquad [2]$$

(HRW, 2010)

Where:

f = Frequency (Hz)
R = Resistance (Ω)
C = Capacitance (F)

In an RLC Circuit, current can be found by:

$$i = \frac{V}{\sqrt{R^2 + (2\pi f L - \frac{1}{2\pi f C})^2}} \qquad [3]$$

(HRW, 2010)

Where:

i = Current (A)
L = Inductance (H)

This function will have a frequency where current is maximized. This is given by:

$$f = \frac{1}{2\pi\sqrt{LC}} \quad [4]$$

(HRW, 2010)

For any of these circuits that peak at such a frequency, a bandwidth can be derived:

$$f_B = \frac{R}{2\pi L} \quad [5]$$

(HRW, 2010)

Where:

f_B = Bandwidth (Hz)

The Biot-Savart Law is used when calculating magnetic fields:

$$d\vec{B} = \frac{\mu_0}{4\pi}\frac{id\vec{l}\times\hat{r}}{r^2} \quad [6]$$

(van Bemmel, 2017)

Where:

$d\vec{B}$ = Differential of magnetic field (T)
$d\vec{l}$ = Differential length of a section (m)
r = Distance from reference point (m)

III Method

A simple series RC circuit was constructed using a resistance of (9.955±.008)Ω and capacitance of (220±5)µF. The oscilloscope measured the potential of the function generator and across the resistor. This allowed the production of a Lissajous figure of the two potentials. Because Ohm's Law gives a relationship between potential and current, the potential across the resistor can be taken as representative of the current (HRW, 2010).

A (98.1±.9)nF capacitor, a (10.0±.8)mH inductor, and an arrangement of resistors with total resistance (48.6±.4)Ω were then connected in series with the function generator. This function generator's impedance was measured to be (49.6±.4)Ω, and so the resistor value was chosen to approximately match it. Values for potential were taken across the resistor setup using a multimeter. From [4] and the given values, a theoretical natural frequency of (5100±200)Hz was predicted. Based on this, points were manually taken across frequencies ranging from 100Hz to 10,000kHz, verified by the digital oscilloscope.

The transformer that was created was made with an input coil with 300 turns of wire and an output coil with 1200 turns, resulting in a step-up transformer with a theoretical amplification factor of 4. The core of the transformer was made of laminated steel. It was constructed with a U-shaped piece with an I-shaped piece stacked on top. The input side of the coil was connected to a function generator. The oscilloscope was then connected to both sides of the transformer so that both the input and output potentials could be measured. Values were measured at arbitrary frequencies, scaled logarithmically and additional data points were taken near the maximum output voltage.

The solenoid was powered by a (1.51±.04)V battery. A ruler was placed along the longitudinal axis, measuring the one edge of the solenoid at the 0 cm mark. The exact position of the probe sensor was found at a point away from very tip of the probe itself. This was taken into account by positioning the sensor, rather than the tip, on a ruler mark. The probe was oriented parallel to the longitudinal axis, along which the B field intensity was measured. The ambient B field was also measured and subtracted from the obtained measurements to obtain the true values.

Two solenoids were given arbitrary positions and rotational elements. The positions were taken about the centre of each solenoid, and rotation was recorded CCW along each axis. Props were used to achieve the desired rotational positions, with each prop height calculated using trigonometry and angles set using a protractor. 10 separate points were recorded. Eight points were observed in the form of a 3x3x3 cm cube between the two solenoids. Additional points were observed on each of the open faces of the solenoids that faced towards the cube. The ambient B field was measured in a similar manner.

IV Analysis

To analyze the RC phase shift, equations for the potential and current waveforms must be constructed. The data below was measured using the digital oscilloscope.

	Frequency (Hz)	Amplitude (V)	Phase Shift (s)
V_{Souce}	(14.7 ± .4)	(3.6 ± .1)	(0.050 ± .002)
$V_{Resistor}$	(14.7 ± .4)	(0.76 ± .02)	(0.0354 ± .001)

Fig 1.0. The data chart for values measured by the oscilloscope. This data is taken from a chart of 2500 points from the oscilloscope. Uncertainties follow the official specifications.

A resistance of (9.955 ± .008)Ω was used. For simplicity, the reading was set to have no vertical shift in the oscilloscope. From Ohm's Law, potential and current are proportional (HRW, 2010), and the x variable time is independent of potential and current, thus allowing the analysis of the potential across the resistor in place of the current waveform. From [1], the equation of the sinusoidal waveform modeling the potential can be constructed as:

$$V_S = (3.6 \pm .1)\sin((14.7 \pm .4)t - (0.050 \pm .002)) \quad [7]$$

$$V_R = (0.76 \pm .02)\sin((14.7 \pm .4)t - (0.0354 \pm .001)) \quad [8]$$

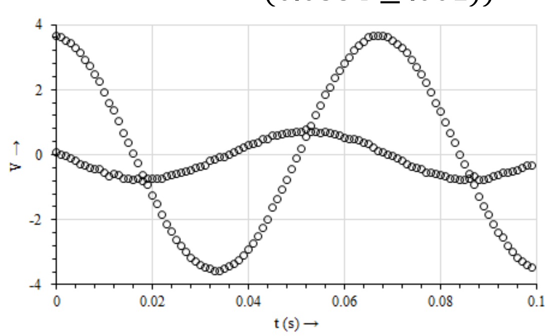

Fig 1.1. Sinusoidal functions [7] and [8]. The data points shown are from the original 2500 data points, taken at intervals for a cleaner presentation. Error lies within the points, and is thus left out.

From the two waveforms, the phase difference can be calculated by subtracting the two horizontal shifts, giving a phase shift (0.0146 ± .002)s with the $V_{Resistor}$ waveform leading.

Frequency and period have an inverse relationship (HRW, 2010), thus, using the inverse frequency, a ratio to degrees equivalent to a (77.263 ± .002)° phase shift is obtained. From [2], a theoretical phase shift of (79 ± 3)° is expected, closely matching the experimental. Since the phase difference was given by a time value, it is independent of the RC components. This means that all RC circuits contain a phase difference. In fact, an ideal RC circuit contains a shift of 90° ("The RC Oscillator", 2017) . To verify the RC circuit from "Lab 3: DC Transients and Semiconductors", the previous data is taken. With a resistance of (1000 ± 10)Ω and a capacitance of (470 ± 5)µF, and setting a frequency of (14.7 ± .4) equalled to the above experiment, [2] can be used to predict a theoretical phase shift of (1.32 ± .04)°. This is miniscule, and any higher frequencies would only yield lower angles. Hence, more suited values were chosen for this experiment.

Plotting the corresponding Lissajous figure for 1 period, its elliptical nature can be seen. From the data, a slight slant of the top right corner favouring quadrant 1 can be seen, predicting a phase difference of 0°<ϕ<90°.

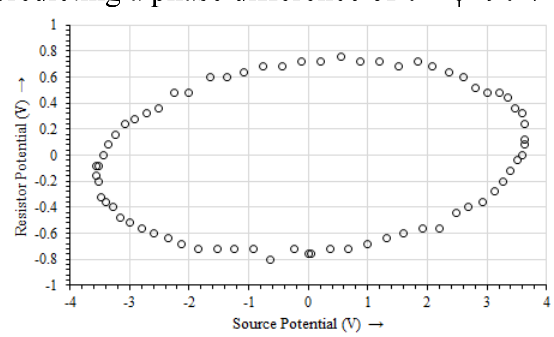

Fig 1.3. The Lissajous figure for the sinusoidal waveform plotting [7] vs [8]. Individual data points were taken at interval of the original 2500 points for a cleaner presentation. Error lies within the points, and is thus left out.

To analyze a series RLC Circuit, current amplitude can be stated as a function of frequency by [3]. Measurements of potential over the resistor through different frequencies were compared to a theoretical function derived from given resistance, capacitance, and inductance. Based on [3], current in the circuit would be maximized when the reactances of the capacitor and inductor cancelled out, and the impedance of the circuit would match that of the source (McHutcherson, 2013). To find a maximum frequency in the experimental data, extrapolation was used, as it was not possible to conduct a proper regression in the function [3]. This maximum was found at a frequency of (5010±30)Hz. From [4], the resonant frequency is (5100±200)Hz. This experimental peak was within a margin of error.

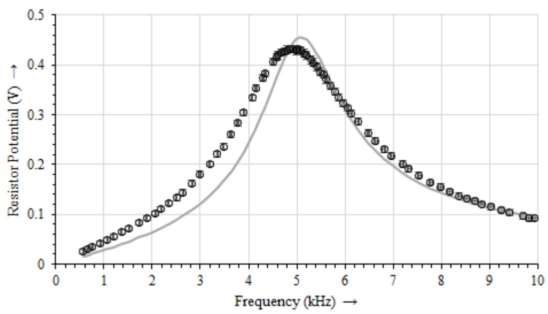

Fig 2.0 Plot of potential over resistor as a function of frequency. A line which represents the theoretical function of [3] is compared to the measured data points. As potential is measured over a resistor, it is proportional to current.

Additionally, for both of these curves, a bandwidth was calculated. Using [5], theoretical bandwidth would be (1600±100) Hz. From the data that was measured, bandwidth was found by determining the points at which the amplitude equaled the maximum amplitude multiplied by a factor of 0.707. The points were found on the graph, and a bandwidth was measured using the difference between two points, yielding a value of (2220±40) Hz. Despite the similarities in the resonant frequencies, there was a larger discrepancy here: the measured bandwidth was (140±10)% of the theoretical bandwidth.

From the compared graphs, it can be said that the capacitor in the circuit worked differently than expected. From [3], at frequencies lower than the resonant frequency, the lower current is caused by an increased reactance of the capacitor, and at higher frequencies, by the reactance of the inductor. In the graph, the measured amplitude points followed the theoretical curve after the resonant frequency, indicating that the inductive reactance was increasing in an expected manner. However, the measured points before are all consistently higher than the theoretical current, which implies that the reactance of the capacitor was lower than expected at lower frequencies. This was likely due to the low capacitance and resistance values used; the capacitor would likely take a miniscule amount of time to fully charge at lower frequencies, likely lower than the period. If the capacitor charges fully before the current changes direction, it essentially acts as an open circuit for that amount of time, and this means that more current is allowed through the circuit. For this reason, ceramic capacitors are mainly designed for high frequency applications. This is likely the effect that caused the consistently higher measured current and the higher bandwidth.

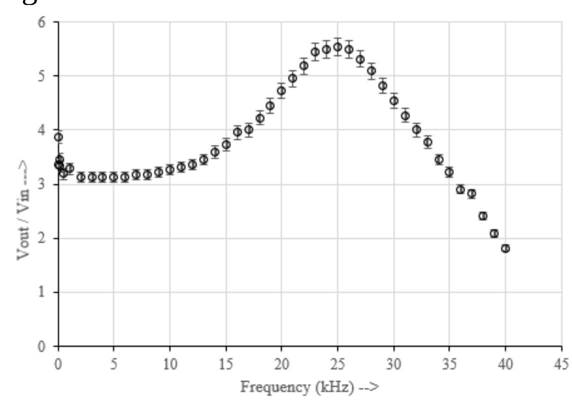

Fig 3.0 The plot of the ratio of the output potential to input potential of the transformer (V_{OUT}/V_{IN}) vs the frequency. The plot shows that initially the ratio follows the expected N_S/N_P of 4, it then drops suddenly and proceeds to rise to its peak of (6.1±.02)V at a frequency of (24.9±.2)kHz.

The potential peaked to (6.1±.02)V at a frequency of (24.9±.2)kHz. The considerable drop began after this point. An effect that can be the cause of this is the skin effect, which is caused by to opposing eddy currents that form due to the changing magnetic field in AC circuits. It causes the current density to be unevenly distributed throughout the wire, with more current flowing near the perimeter or skin of the wire. With higher frequency the skin becomes thinner and the cross-section of the wire is reduced. A lower cross-sectional area in a wire leads to an increased resistance (HRW 2010). That increased resistance is what causes the potential to decrease since more power is lost via heat.

The other consideration for the potential drop is within the transformer core. The skin effect also occurs with the core and so heat is lost from the core as well. The core also loses energy via heat due to the hysteresis effect. This effect states that when there is a changing magnetic field through the core, the dipoles attempt to align with the field. Work is done for the dipoles in the core to reverse, and the core dissipates energy as heat. The alternating current creates an rapidly varying field and the is a lag effect between dipoles. This creates a friction between them and that is why work is required and heat is created. It is also notable that increasing the frequency causes this effect to be greater.

Although it is possible for each of these energy loss effects to be modeled and calculated to show where the losses occur, due to the non-circular shape of the windings and the rectangular core, as well as the flux losses in the induction process, any attempt at modeling was deemed to be too inaccurate to continue pursuing.

The peak of the magnetic field curve is located at the centre of the solenoid (3.50±.05 cm). The sensor is minimizing the average distance to all the current-carrying coils, increasing the magnetic flux density. Moving away from the centre, the curve concaves down. The slope starts off mild because while the sensor moves away from some of the coils, it is also moving towards other coils. As the sensor moves further from the centre, it begins to move away from more coils and move towards less. This creates the negative concavity of the curve. However, when the sensor is outside of the solenoid, any further displacement moves it further from all the coils. [6] follows the proportionality of the inverse square law. As such, the decrease in flux density slows down as the density approaches 0.

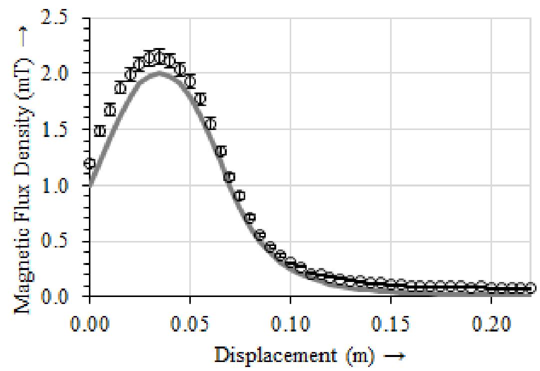

Fig 4.0. Observed vs. calculated magnetic flux densities with relation to displacement. The solid line represents the calculated values while the points represent measured entities.

While the simulated magnetic field approaches, the measured magnetic field appears to stay above a certain threshold. This points to a different source of magnetism, likely the ambient magnetic field. Although this was considered, the measurement fluctuated during recording and could have been recorded as an untrue value. However, this does not explain the larger discrepancy near the peak of the curve. This is thought to be an equipment fault. The discrepancy is larger at the peak and decreases when the magnetic flux density decreases, indicating that it correlates to the magnitude of the magnetic field itself. This “multiplying element” cannot be a different source of magnetic flux due to superpositioning. It is much more likely to be the sensor itself that led to the differences between observed measurements and computed values.

The flux density is highest near each solenoid. In between them, the magnitude is reduced since their magnetic fields superimpose, opposing each other. Both sets of points follow the same trend, indicating

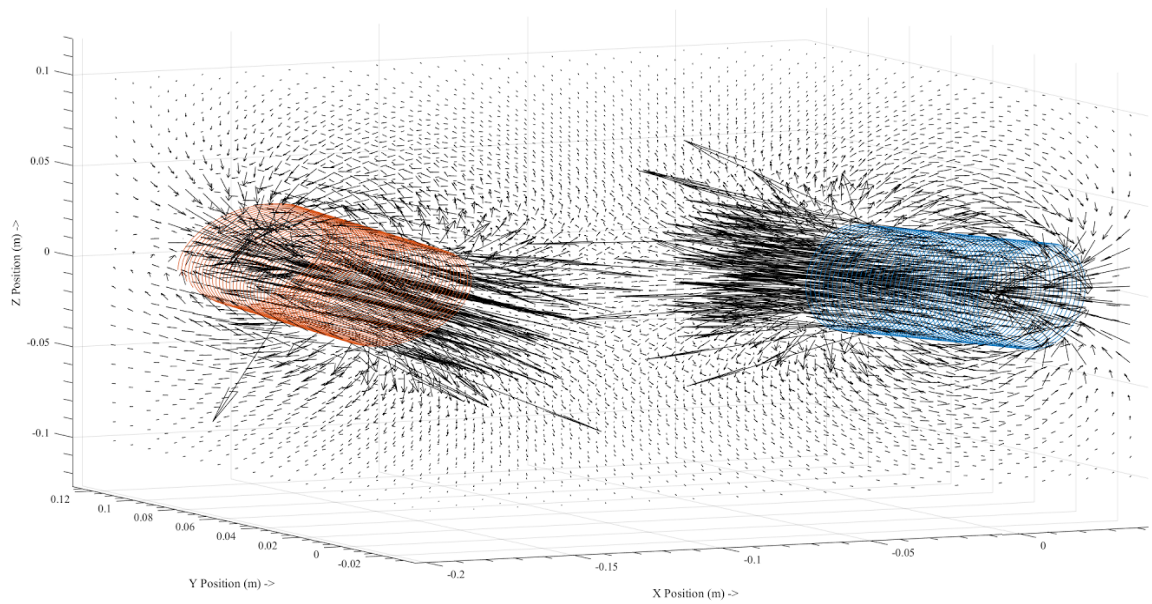

Fig 5.0. Visual representation of magnetic field in 3D space. A vector field is plotted using MATLAB and [6].

that the simulation is valid. However, the values are discrepant.

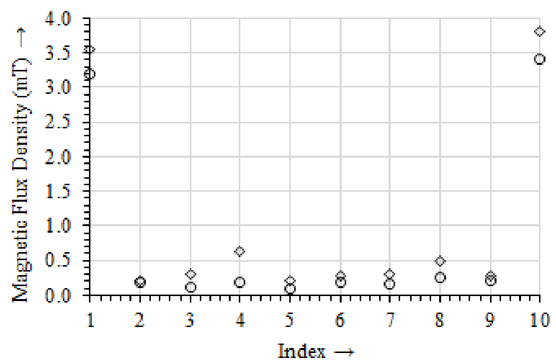

Fig 5.1. Plot of theoretical vs. measured B magnitudes. Circles represent the experimental data, while diamonds represent the theoretical values.

This error is likely due to a combination of human error and the nature of the simulation. Three-dimensional space is difficult to be accurate in. Hence, displacement measurements may not be consistent. Also, for the sake of simplicity, the simulation approximates the coil as a series of points arranged in a helix. This neglects the "rounded square" shape of the solenoid that was used. Although coils are symmetrical, readings taken near the corners of the solenoids may be inaccurate.

V Conclusion

Through the analysis of various circuits in AC, theoretical and experimental phase shifts between potentials, resonant frequencies, and bandwidths were compared. Dissipation of energy via heat was noted in a transformer at higher frequencies. Additionally, magnetic fields of simple solenoids were measured. Despite some disparity in bandwidth and magnetic fields, measured properties correlated with theoretical values. For future experimentation, usage of higher-quality capacitors and probes would likely increase accuracy of readings, as would more careful management of other components.

VI Sources

(n.d.). Retrieved December 18, 2017, from http://www.electronics-tutorials.ws/oscillator/rc_oscillator.html

van Bemmel, H. "Laboratory Manual", Retrieved from http://www.hmvb.org/apc1718lm.pdf, 2017

van Bemmel, H. "Biot-Savart Primer", Retrieved from http://www.hmvb.org/biotsavart.pdf, 2017

Berglund, R. (2009). Frequency Dependence of Transformer Losses.

Halliday, D., Resnick, R., & Walker, J. (2010). WP Course Fundamentals of Physics Extended, 9th Edition. John Wiley & Sons.

McHutcherson, A. (2013). RLC Resonant Circuits. Unpublished manuscript.